

# Why are some BL Lacs detected by *Fermi* , but others not ?

Zhongzu Wu <sup>★1</sup>, D. R. Jiang<sup>2</sup>, Minfeng Gu<sup>2</sup>, Liang Chen<sup>2</sup>

<sup>1</sup> College of Science, Guizhou University, Guiyang 550025, China.

<sup>2</sup> Key Laboratory for Research in Galaxies and Cosmology, Shanghai Astronomical Observatory, Chinese Academy of Sciences, 80 Nandan Road, Shanghai 200030, China

Received / Accepted

**Abstract.** By cross-correlating an archival sample of 170 BL Lacs with 2 year *Fermi*/LAT AGN sample, we have compiled a sample of 100 BL Lacs with *Fermi* detection (FBLs), and a sample of 70 non-*Fermi* BL Lacs (NFBLs). We compared various parameters of FBLs with those of NFBLs, including the redshift, the low frequency radio luminosity at 408 MHz ( $L_{408\text{MHz}}$ ), the absolute magnitude of host galaxies ( $M_{\text{host}}$ ), the polarization fraction from NVSS survey ( $P_{\text{NVSS}}$ ), the observed arcsecond scale radio core flux at 5 GHz ( $F_{\text{core}}$ ) and jet Doppler factor; all the parameters are directly **measured** or derived from available data from literatures. We found that the Doppler factor is on average larger in FBLs than in NFBLs, and the *Fermi*  $\gamma$ -ray detection rate is higher in sources with higher Doppler factor. In contrast, there are no significant differences in terms of the intrinsic parameters of redshift,  $L_{408\text{MHz}}$ ,  $M_{\text{host}}$  and  $P_{\text{NVSS}}$ . FBLs seem to have a higher probability of exhibiting measurable proper motion. These results strongly indicate a higher beaming effect in FBLs compared to NFBLs. The radio core flux is found to be strongly correlated with  $\gamma$ -ray flux, which remains after excluding the common dependence of the Doppler factor. At the fixed Doppler factor, FBLs have systematically larger radio core flux than NFBLs, implying lower  $\gamma$ -ray emission in NFBLs since the radio and  $\gamma$ -ray flux are significantly correlated. Our results indicate that the Doppler factor is an important parameter of  $\gamma$ -ray detection, the non-detection of  $\gamma$ -ray emission in NFBLs is likely due to low beaming effect, and/or low intrinsic  $\gamma$ -ray flux, and the gamma-rays are likely produced co-spatially with the arcsecond-scale radio core radiation and mainly through the SSC process.

**Key words.** BL Lacertae objects: general – galaxies: active – galaxies: jets – galaxies: nuclei – radio continuum: galaxies

## 1. Introduction

Blazars are an extreme subclass of AGNs with characteristic properties such as rapid variability at all wavelengths, high optical polarization, apparent superluminal motion, flat radio spectra, and a broad continuum extending from the radio through the  $\gamma$ -rays (Urry & Padovani 1995). The distinctive characteristic of blazars is a relativistic jet oriented close to our line-of-sight. BL Lac objects are blazars with only very weak or non-existent emission lines (equivalent width  $< 5 \text{ \AA}$ ; e.g., Scarpa & Falomo 1997).

They can be classified as different subclasses based on the synchrotron peak of their spectral energy distribution (SED), namely, low-frequency peaked BL Lac objects (LBL), intermediate objects (IBL) and high frequency peaked BL Lac objects (HBL) (Padovani & Giommi 1995). The boundaries used for this work are as follows: for LBLs,  $\log \nu_{\text{peak}} < 14.5$ , for IBLs  $14.5 < \log \nu_{\text{peak}} < 16.5$ , and for HBLs  $\log \nu_{\text{peak}} > 16.5$  (Nieppola et al. 2006). The Large Area Telescope (Atwood et al. 2009, LAT) on board the *Fermi*  $\gamma$ -ray Space Telescope has been scanning the entire  $\gamma$ -ray sky approximately once every three hours since July of 2008. The LAT AGN catalogs

(Abdo et al. 2009, 2010; Ackermann et al. 2011) have shown that BL Lac objects have been the most numerous group of  $\gamma$ -ray sources. The most recent LAT AGN catalog is the LAT Second Catalog of AGN (2LAC; Ackermann et al. 2011), the Clean Sample (sources with single associations and not affected by analysis issues) includes 310 FSRQs, 395 BL Lacs, 24 other AGNs, and 157 of unknown type, which makes it possible to study the statistical properties of  $\gamma$ -ray sample of BL Lac objects.

By now, several possible answers have been proposed to the question “why are some sources  $\gamma$ -ray loud and others are  $\gamma$ -ray quiet?”. Doppler boosting is believed to be one of the important answers for this question. Piner et al. (2012) showed that sources in the *Fermi* LAT Second Source Catalog (2FGL; Nolan et al. 2012) display higher apparent speeds than those that have not been detected. Pushkarev et al. (2012) also showed that the *Fermi* AGNs have higher VLBI core flux densities and brightness temperatures, and are characterized by the less steep radio spectrum of the optically thin jet emission. Linford et al. (2011, 2012) showed that the LAT flat-spectrum radio quasars (FSRQs) are significantly different from the non-LAT FSRQs, while the *Fermi* detected BL Lacs (FBLs) tend to be generally similar to the non-*Fermi* BL Lacs (NFBLs); for ex-

★ e-mail: zzwu08@gmail.com

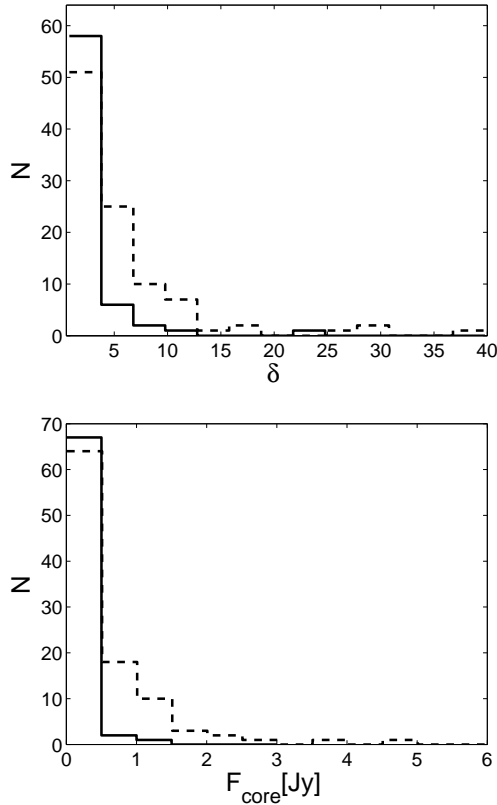


**Fig. 1.** The distributions of Doppler factor  $\delta$  (top) and radio core flux  $F_{\text{core}}$  (bottom) for our BL Lacs. The dashed lines are for FBLs, while the solid lines for NFBLs.

ample, there are no differences in the fraction of polarized BL Lac objects or the distributions of the polarization. Irrespective of the general similarity, some differences between FBLs and NFBLs have been found. Linford et al. (2011, 2012) reported that the FBLs have longer jets, and are polarized more often, but core polarization itself seems not enough to separate two populations. Alternatively, the NFBLs may enter a state where  $\gamma$ -ray production ceases or is at least significantly reduced. However, the sample size of NFBLs in Linford et al. (2012) is rather small compared to FBLs, their results may not be conclusive.

In this work, in order to better understand the question “why are some sources  $\gamma$ -ray detected and others are not?”, we compared various parameters of *Fermi* BL Lacs (FBLs) with those of non-*Fermi* BL Lacs (NFBLs) selected from cross-correlating the sample of 170 BL Lacs in Wu et al. (2007) with 2LAC AGN sample. The organization of this paper is as follows: the sample selection is presented in section 2; the comparisons of FBLs and NFBLs are shown in section 3; the discussions are given in section 4, and the results are summarized in section 5. Throughout the paper, we define the spectral index  $\alpha$  as  $S_\nu \propto \nu^{-\alpha}$ , where  $S_\nu$  is the flux density at frequency  $\nu$ , and a cosmology with  $H_0 = 70 \text{ km s}^{-1} \text{ Mpc}^{-1}$ ,  $\Omega_M = 0.3$ ,  $\Omega_\Lambda = 0.7$  (e.g. Hinshaw et al. 2009) is adopted.

## 2. The sample

Nieppola et al. (2006) presented a large sample of BL Lac objects, and the authors argued that this sample is supposed to have no selection criteria (other than declination) in addition to the ones in the original surveys. From this sample, Wu et al. (2007) estimated the Doppler factor for a sample of 170 BL Lac objects using  $P_{\text{co5}} = P_{\text{ci5}} \delta^{2+\alpha}$  and  $\log P_{\text{ci5}} = 0.62 \log P_t + 8.41$  derived for radio galaxies in Giovannini et al. (2001), in which  $P_{\text{co5}}$  is the observed 5 GHz core luminosity,  $P_{\text{ci5}}$  is the intrinsic 5 GHz core luminosity, and  $P_t$  is the total radio luminosity at 408 MHz (see Wu et al. 2007, for details).

By cross-correlating the sample of 170 BL Lacs in Wu et al. (2007) with 2LAC, we define a subsample of 100 BL Lacs as FBLs sample, which were all detected with *Fermi* LAT. The remaining 70 BL Lacs are included in NFBLs sample, as they were not detected with *Fermi* LAT. Linford et al. (2012) selected samples of FBLs and NFBLs based on available VLBI images, in which the median values of the total VLBA flux density at 5 GHz are 177 mJy for FBLs and 221 mJy for 24 NFBLs, respectively. Compared to Linford et al. (2012) sample, the median flux density of our sample is much lower (see Table 1), especially for NFBLs, and the number of our NFBLs is about three times larger than theirs.

## 3. The properties of FBLs and NFBLs

To explore the differences of FBLs and NFBLs, we compare various properties for two subsamples, including the redshift, the low frequency radio luminosity at 408 MHz ( $L_{408\text{MHz}}$ ), the absolute magnitude of host galaxies ( $M_{\text{host}}$ ), the polarization fraction from the NRAO VLA Sky Survey (NVSS) survey ( $P_{\text{NVSS}}$ ), the observed arcsecond scale radio core flux at 5 GHz ( $F_{\text{core}}$ ) and jet Doppler factor. The results are shown below.

### 3.1. The distributions for $z$ , $L_{408\text{MHz}}$ , $M_{\text{host}}$ , $P_{\text{NVSS}}$

We compared several intrinsic parameters in FBLs with NFBLs, including redshift  $z$ ,  $L_{408\text{MHz}}$ ,  $M_{\text{host}}$ , and  $P_{\text{NVSS}}$ . The redshift is available in 159 BL Lacs from NED<sup>1</sup> and new measurements in Shaw et al. (2013), including 81 FBLs, and 68 NFBLs. The  $L_{408\text{MHz}}$  of all sources are directly adopted from Wu et al. (2007), which is the available arcsecond scale extended flux or was estimated from the radio flux at nearest frequency. The  $L_{408\text{MHz}}$  is expected to be less influenced by beaming effect because it is comparable with  $L_{408\text{MHz}}$  of FR I radio galaxies (Wu et al. 2007).  $M_{\text{host}}$  is available in Wu et al. (2009) for 121 BL Lacs, including 69 FBLs and 52 NFBLs. We collected the fraction of the polarized flux in total flux  $P_{\text{NVSS}}$  from NVSS, which is available for 92 FBLs and 55 NFBLs. The Kolmogorov Smirnov (KS) test shows that the distributions of FBLs and NFBLs do not show significant differences for all four parameters (see Table 1). However, the  $\chi^2$ -test does not show similarities between FBLs and NFBLs in the distributions of all four parameters.

<sup>1</sup> <http://ned.ipac.caltech.edu/>

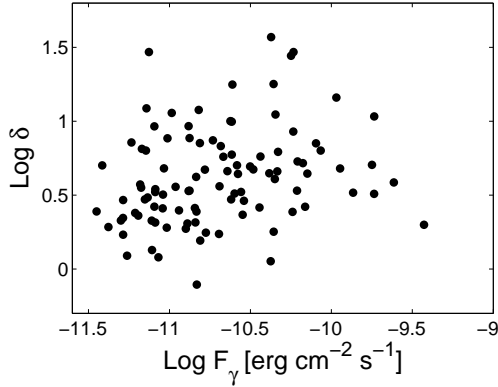


**Fig. 2.** The  $\gamma$ -ray flux versus Doppler factor for FBLs.

### 3.2. The Doppler factor and radio core flux

The Doppler factor  $\delta$  can directly measure the significance of jet beaming effect, and the radio core flux usually are boosted by jet beaming effect in BL Lacs (Wu et al. 2007). These two parameters are available for all 170 BL Lacs in Wu et al. (2007). In Fig. 1, we compare the distributions of Doppler factor and the radio core flux  $F_{\text{core}}$  for all BL Lacs. We found that FBLs on average have larger Doppler factor  $\delta$  and larger  $F_{\text{core}}$  than NFBLs. The KS test shows that there are significant differences between the total samples of FBLs and NFBLs in distributions of Doppler factor and  $F_{\text{core}}$ , all at the confidence level larger than 99.99% (see Table 1). The systematically higher mean and median radio core flux in FBLs indicates that the intrinsic radio core flux may be higher than that in NFBLs at the fixed Doppler factor.

### 3.3. The $\gamma$ -ray flux and Doppler factor

We collected the  $\gamma$ -ray flux  $F_\gamma$  in the 100 MeV to 100 GeV range for all 100 FBLs from 2FGL. We show the relation between  $F_\gamma$  and  $\delta$  in Fig. 2. By using Spearman rank correlation analysis (Macklin 1982), we found a significant correlation between the Doppler factor and  $F_\gamma$  with correlation coefficient  $r = 0.296$  at  $> 99\%$  confidence level. A strong correlation ( $r=0.365$  at  $> 99.9\%$  confidence level) is also found between  $\delta$  and  $\gamma$ -ray luminosity  $L_\gamma$ . These results indicate that  $\gamma$ -ray emission is severely influenced by jet beaming effect. The Doppler factor is likely an important factor responsible for the detection of *Fermi* BL Lacs.

## 4. Discussion

BL Lac objects are believed to be beamed FR I radio galaxies, and their multi-band electromagnetic radiation are related to the presence of relativistic particles in jets. Beaming is an important effect for understanding this type of objects. From a large sample of BL Lacs with estimated Doppler factor (Wu et al. 2007), we have found significant difference in Doppler factor of FBLs and NFBLs, while no significant differences in terms of several intrinsic parameters  $z$ ,  $L_{408\text{MHz}}$ ,  $M_{\text{host}}$ , and  $P_{\text{NVSS}}$ . The Doppler factor of FBLs are systematically higher

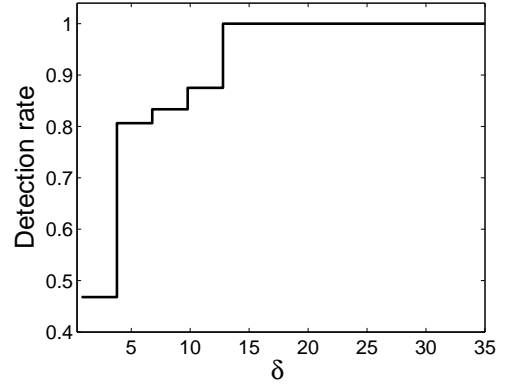


**Fig. 3.** The *Fermi*  $\gamma$ -ray detection rate and Doppler factor.

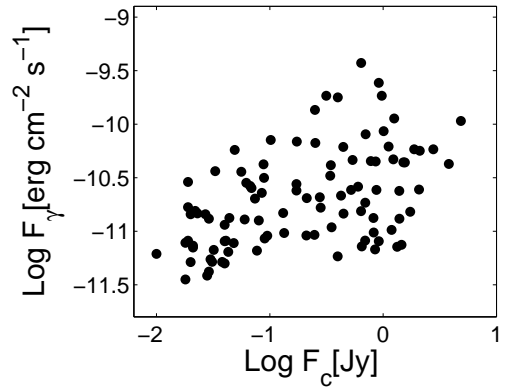


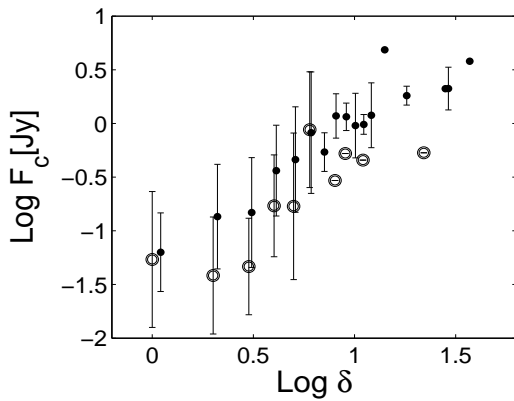
**Fig. 4.** The relation between radio core flux at 5 GHz and  $\gamma$ -ray flux in the 100 MeV to 100 GeV range.

than those of NFBLs, implying important role of jet beaming effect in  $\gamma$ -ray detection. This systematic difference is also evident in the subsamples of LBLs and IBLs (see Table 1), but not in HBLs. However, the small number of sources precludes us to draw any firm conclusions in each subsamples. Savolainen et al. (2010), using a sample consisting mostly of FSRQs and a different method of calculating the Doppler factor, reported a similar result in that *Fermi*-detected sources had larger Doppler factors, on average. In Fig. 3, we plot the *Fermi*  $\gamma$ -ray detection rate (i.e. the ratio of the FBLs number to total BL Lacs in bins of Doppler factor, in which we use 3 as bin in Doppler factor) versus the Doppler factor. We found that the detection rate increases with Doppler factor when  $\delta < 10$ , and it reaches 1.0 at  $\delta > 10$  and remains all the way to high  $\delta$  values. This implies that sources with smaller Doppler factor may have smaller probability to have significant  $\gamma$ -ray emission.

Proper motions can be used to study the bulk motion of jets when combining with other measurements. The superluminal motion have been often observed in blazars with relativistic jets moving towards us at small viewing angle. Piner et al. (2012) showed that sources in 2FGL display higher apparent speeds than those that are not detected by *Fermi*. We have searched literatures and found proper motion measurements for 38 sources, consisting of 33 FBLs and 5 NFBLs

**Table 1.** The KS test on properties of *Fermi* and non-*Fermi* BL Lacs

Parameter	KS statistic	probability	Significantly different	subsets	$N_{\text{FBLs}}$	$N_{\text{NFBLs}}$	mean/median (FBLs)	mean/median(NFBLs)
$z$	0.111	0.704	NO	allBLs	93	66	0.41/0.30	0.35/0.30
$\delta$	0.469	1.29e-08	YES	allBLs	100	70	5.8/3.7	2.9/2.1
	0.412	0.013	YES	LBLs	50	19	8.8/6.4	5.3/3.7
	0.583	2.73e-04	YES	IBLs	24	24	3.4/3.3	2.1/2.0
	0.319	0.107	NO	HBLs	26	27	2.5/2.2	1.9/1.9
$\text{Log } L_{408 \text{ MHz}}$	0.187	0.099	NO	allBLs	100	70	25.6/25.5	25.1/25.1
$P_{\text{NVSS}}$	0.146	0.438	NO	allBLs	94	53	2.27/2.11	2.81/2.08
$M_{\text{host}}$	0.210	0.132	NO	allBLs	71	50	-22.9/-23.1	-23.0/-23.2
$F_{\text{core}}$	0.306	6.52e-04	YES	allBLs	100	70	0.55/0.23	0.10/0.023

**Fig. 5.** The relation between the Doppler factor and the average radio core flux in binned  $\delta$ , with errorbars showing the standard deviation of core flux in each bin. The solid and open circles stand for FBLs and NFBLs, respectively.

(see Table 3). Therefore, the measurements rate of proper motion are  $\sim 34\%$  and  $\sim 7\%$  for FBLs and NFBLs, respectively. Because the source selection for proper motion observations is usually not relevant with the information of  $\gamma$ -ray detection, so the available proper motion is hardly biased toward FBLs. The higher proper motion measurement rate in FBLs implies that the proper motion might be easier to be detected in FBLs, likely due to the higher jet beaming effect, thus consistent with higher Doppler factor in FBLs or the NFBLs are intrinsically dimmer.

#### 4.1. The radio core flux and $\gamma$ -ray detection of BL Lacs

Because  $\gamma$ -ray flux and radio core flux are Doppler boosted, a strong correlation between them is expected, which is plotted in Fig. 4. Indeed, a significant correlation is found with Spearman correlation coefficient  $r = 0.493$  at  $\gg 99.99\%$  level. Interestingly, the correlation is still significant even after excluding the common dependence on the Doppler factor by using the partial Spearman correlation method (Macklin 1982), with a correlation coefficient of 0.429 at  $\gg 99.99\%$  level. To further study the nature of NFBLs, we investigate the differences of FBLs and NFBLs in radio core flux at fixed Doppler factor. In Fig. 5, we show the relationship between  $\delta$  and the average  $F_{\text{core}}$  of FBLs and NFBLs in  $\delta$  bins, in which we

use 1 as the bin size in  $\delta$ . Intriguingly, FBLs have systematically larger radio core flux than NFBLs at fixed  $\delta$ , indicating larger intrinsic radio core flux in FBLs. By separating our 100 FBLs into two subsamples based on their  $\gamma$ -ray flux: 50 FBLs with relatively high  $\gamma$ -ray flux (HG-FBLs) (larger than  $1.7 \times 10^{-11} \text{ erg/cm}^2/\text{s}$ ) and others with relatively lower  $\gamma$ -ray (LG-FBLs), we also investigated the differences of HG-FBLs and LG-FBLs in radio core flux at fixed Doppler factor similar as we did for FBLs and NFBLs; the result is also similar with FBLs and NFBLs as showed in Fig. 5, which means that HG-FBLs also have systematically larger radio core flux than LG-FBLs at fixed  $\delta$ , indicating larger intrinsic radio core flux in HG-FBLs. In combination with the correlation between  $F_{\text{core}}$  and  $F_{\gamma}$ , NFBLs may have relatively smaller  $F_{\gamma}$  even though they have comparable  $\delta$  with FBLs, making them more difficult to be detected by *Fermi* LAT.

From Fig. 5, it can be seen that the radio flux of NFBLs at fixed Doppler factor are systematically lower than FBLs, indicating that the  $\gamma$ -ray flux for NFBLs might also be lower, which likely results non-detection with *Fermi* telescope. Together with difference in  $\delta$ , the non-detection of *Fermi*  $\gamma$ -ray emission in NFBLs is likely due to their smaller Doppler factor and/or lower intrinsic  $\gamma$ -ray flux. However, it should be noticed that the radio flux of NFBLs covers a wide range overall or in each Doppler factor bin as shown by the large errorbar. The investigations on the differences between FBLs and NFBLs are further complicated due to the fact that BL Lac objects usually exhibit violent variations. Because the  $\gamma$ -ray and radio emission were not observed simultaneously, the variations thus may be at least partly responsible for the large dispersion of correlation between the  $\gamma$ -ray and radio flux (see Fig. 4). It is highly possible that NFBLs may enter a state where  $\gamma$ -ray production ceases or is at least significantly reduced (Linfood et al. 2012). To exclude the effect of variations, the simultaneous observations at  $\gamma$ -ray and other wavebands are required for larger samples of BL Lac objects, especially at radio bands.

There are two popular models for the  $\gamma$ -ray emission mechanism of blazars, the synchrotron self-compton model (SSC, seed photons from synchrotron radiation) and external-radiation-Compton (ERC, seed photons from external region) (Chen & Bai 2011). Typically, ERC scenario requires that the inverse Compton (IC) radiation, i.e.,  $\gamma$ -rays, originate relatively close to center, within central parsec, while SSC  $\gamma$ -rays come from jets beyond a parsec's distance (Nieppola et al.

2011). Our results have shown that the non-detection of  $\gamma$ -ray is likely related with lower intrinsic radio core flux, which is originated from the jet synchrotron emission. The close relations of  $\gamma$ -ray to radio emission may support the view of Nieppola et al. (2011) that  $\gamma$ -rays are produced co-spatially with the arcsecond-scale radio core radiation, indicates that  $\gamma$ -ray is likely produced mainly through the SSC process in our sample.

#### 4.2. Effects of radio variability

BL Lacs are known to show significant and rapid variations at nearly all wavebands. The effects of variations might be non-trivial in our results since the radio and  $\gamma$ -ray emission were not observed simultaneously. Although the  $\gamma$ -ray flux are variable, there should be little concern about short-term variability since the 2FGL data are basically averaged over  $\sim 2$  years. In this section, we only present the effects of radio variability on our statistical results.

The detailed variations on each source are basically unknown, we then have to make assumptions on the source state. We considered 30% or 50% of sources were in elevated state with radio core flux or luminosity at 120% to 200% of the quiescent level. These 30% or 50% of sources were selected in three ways: (1) at highest radio flux; (2) at highest luminosity; (3) as random sources (see Table 2). We recalculated the Doppler factor with newly assigned radio core quiescent flux or luminosity. The KS tests shows that there are still significant differences between FBLs and NFBLs in distributions of Doppler factor and  $F_{\text{core}}$  in all three circumstances (see Table 2). This strongly implies that the variability may not alter our results.

Alternatively, we investigated how much the variations are needed to eliminate the systematical difference between FBLs and NFBLs in  $\delta$  and  $F_{\text{core}}$  distributions. As the  $\delta$  and  $F_{\text{core}}$  for FBLs are on average much higher than NFBLs (see the mean and median values in Table 1), we assume that the differences are totally due to the elevated state in FBLs during radio observation. Based on the mean values (see Table 1), we found that the significant differences disappear (the probability less than 90% from KS test), when we systematically reduce a factor of 1.7 - 1.9 for  $\delta$ , and a factor of 6 - 9 for  $F_{\text{core}}$  for FBLs, respectively. This means that the FBLs are expected to be in a flare state with flux density of a factor of 6 - 9 averagely higher than quiescent state, if the systematical differences between FBLs and NFBLs are completely caused by variations. However, the typical maximum variations are found to be around a factor of two, for individual sources such as BL Lac (Villata et al. 2009), and S5 0716+714 (Rani et al. 2013), or from the light curves of BL Lac objects in University of Michigan Radio Astronomy Observatory (UMRAO) database<sup>2</sup>. Therefore, the systematical differences between FBLs and NFBLs cannot be caused by the variations only.

We further considered core flux variations within a factor of two in each sources, corresponding to  $\delta$  variations within a factor of  $\sqrt{2}$  (Giroletti et al. 2004). We let  $\delta$  of each object to

vary randomly between  $\delta \times \sqrt{2}$  and  $\delta / \sqrt{2}$  with a step size of 1%. The KS tests on one million samples with allocated  $\delta$  values, show that there is still a significant difference between FBLs and NFBLs in the  $\delta$  distribution (confidence level larger than 99.8%). By varying the core flux, a significant difference is also found between FBLs and NFBLs in the  $F_{\text{core}}$  distribution (confidence level larger than 99.9%). We therefore are confident that the variations in the radio core flux will not significantly change our results.

We also tested the strong correlations of  $\delta$ - $F_{\gamma}$ ,  $\delta$ - $L_{\gamma}$  and  $F_{\gamma}$ - $F_{\text{core}}$ , by varying  $F_{\text{core}}$  randomly with a factor within  $[1/2, 2]$ , and  $\delta$  within  $[1/\sqrt{2}, \sqrt{2}]$ . On a million designed FBLs samples, we found that the significant correlations remain in almost all samples.

In summary, we argued that the variations in the radio core flux density will not affect our results, based on above various considerations.

#### 5. Summary

By using the available data from literatures, we have compared various parameters of FBLs with those of NFBLs. We found that the Doppler factor is on average larger in FBLs than in NFBLs, and the *Fermi*  $\gamma$ -ray detection rate is higher in sources with higher Doppler factor. The arcsecond scale radio core flux of NFBLs is on average lower than the FBLs at fixed doppler factor. Our results indicate that the Doppler factor is an important parameter of  $\gamma$ -ray detection. It seems that variations in the radio core flux density will not affect our results. The non-detection of  $\gamma$ -ray emission in NFBLs is likely due to low beaming effect, and/or low intrinsic  $\gamma$ -ray flux and the  $\gamma$ -rays seems to be produced co-spatially with the arcsecond-scale radio core radiation, and is likely produced mainly through the SSC process.

Because our sample is limited by the available archival data, and the estimation of Doppler factor is based on an empirical relation; the future new observational data including redshift, arcsecond scale radio data, and new improved estimations of Doppler factor for larger sample of BL Lac objects will all be useful for further tests of our results. Additionally, the new observations of BL Lac sample with less beaming effect using Very-long-baseline interferometry (VLBI) technique and at other wavelengths will be also important for understanding the nature of BL Lacs, and also helpful for further testing our results.

**Acknowledgements.** We thank the anonymous referee and editor for insightful comments and constructive suggestions, which were greatly helpful in improving our paper. We thank Emmanouil Papastergis for helpful discussions. This work is supported by the 973 Program (No. 2009CB824800), the NSFC grants (No. 11163002, 11073039, 11103060, 11233006, 11173043), and by the Study Abroad Fund from China Scholarship Council (No.[2011]5024).

#### References

- Abdo, A. A., Ackermann, M., Ajello, M., et al. 2009, *ApJ*, 700, 597

<sup>2</sup> <https://dept.astro.lsa.umich.edu/datasets/umrao.php>

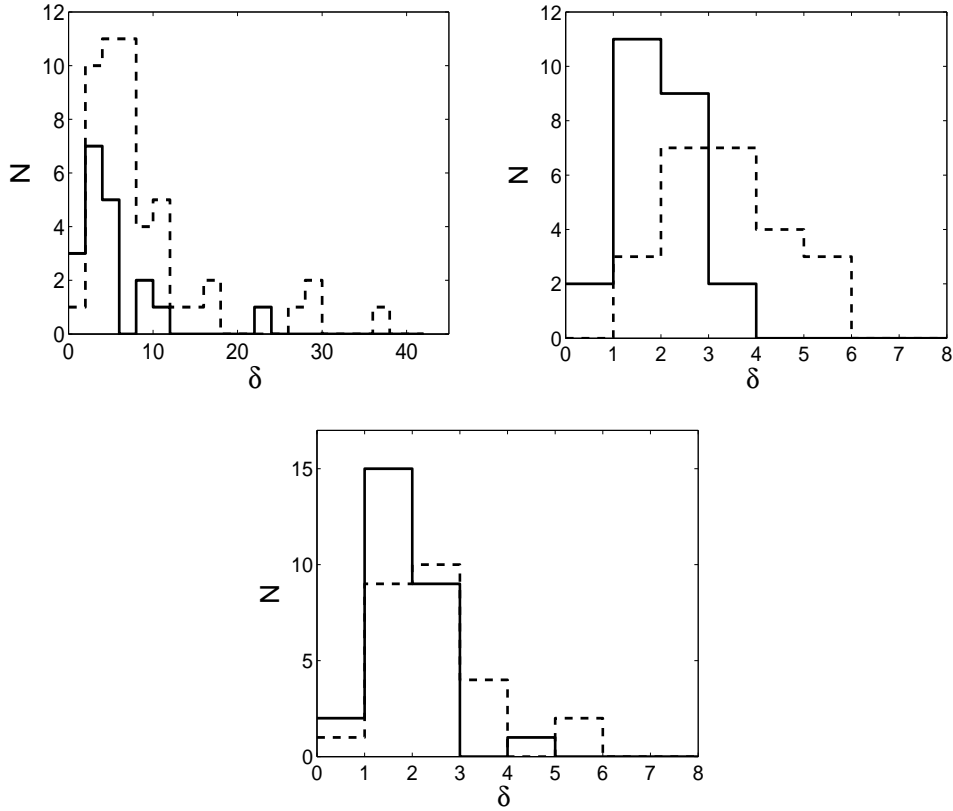
- Abdo, A. A., Ackermann, M., Ajello, M., et al. 2010, *ApJ*, 715, 429
- Ackermann, M., Ajello, M., Allafort, A., et al. 2011, *ApJ*, 743, 171
- Atwood, W. B., Abdo, A. A., Ackermann, M., et al. 2009, *ApJ*, 697, 1071
- Chen, L., & Bai, J. M., 2011, *ApJ*, 735, 108
- Gabuzda, D. C., Pushkarev, A. B., Cawthorne, T. V., 2000, *MNRAS*, 319, 1109
- Giovannini, G., Cotton, W. D., Feretti, L., Lara, L., & Venturi, T. 2001, *ApJ*, 552, 508
- Hinshaw, G., Weiland, J. L., Hill, R. S. et al. 2009, *ApJS*, 180, 225
- Giroletti, M., Giovannini, G., Taylor, G. B., & Falomo, R. 2004, *ApJ*, 613, 752
- Jorstad, S. G., Marscher, A. P., Mattox, J. R., et al. 2001, *ApJ*, 134, 181
- Kellermann, K. I., Lister, M. L., Homan, D. C., et al. 2004, *ApJ*, 609, 539
- Kharb, P., Gabuzda, D., Shastri, P. et al. 2008, *MNRAS*, 384, 230
- Kharb, P., Lister, M. L., Cooper, N. J., 2010, *ApJ*, 710, 764
- Linford, J. D., Taylor, G. B., Romani, R., et al. 2011, *ApJ*, 726, 16
- Linford, J. D., Taylor, G. B., Romani, R., et al. 2012, *ApJ*, 744, 177
- Lister, M. L., Homan, D. C., Kadler, M., 2009, *ApJ*, 696, 22
- Macklin, J.T. 1982, *MNRAS*, 199, 1119
- Nieppola, E., Tornikoski, M., & Valtaoja, E. 2006, *A&A*, 445, 441
- Nieppola, E., Tornikoski, M., & Valtaoja, E. 2011, *A&A*, 535, 69
- Nolan, P. L., et al. 2012, *ApJS*, 199, 31
- Padovani, P., & Giommi, P. 1995, *ApJ*, 446, 547
- Piner, B. G., Bhattarai, D., Edwards, P. G., Jones, D. L., 2006, *ApJ*, 640, 196
- Piner, B. G., Pushkarev, A. B., Kovalev, Y. Y., et al., 2012, *ApJ*, 758, 84p
- Pushkarev, A. B., Kovalev, Y. Y., Lister, M. L., Savolainen, T. 2012, *A&A*, 544, 3p
- Rani, B., Krichbaum, T. P., Fuhrmann, L., et al. 2013, *A&A*, 552, 11R
- Savolainen, T., Homan, D. C., Hovatta, T., et al., 2010, *A&A*, 512, A24
- Shaw, M. S., Romani, R. W., Cotter, G., et al. 2013, *ApJ*, 764, 135S
- Urry C. M., Padovani P., 1995, *PASP*, 107, 803
- Villata, M.; Raiteri, C. M.; Larionov, V. M.; et al. 2009, *A&A*, 501, 455
- Wu, Z. Z., Jiang, D., R., Gu, M. F., Liu, Y., 2007, *A&A*, 466, 63
- Wu, Z. Z., Gu, M. F., Jiang, D., R., 2009, *RAA*, 9, 168
- Wu, Z. Z., Gu, M. F., Jiang, D., R., 2012, *MNRAS*, 424, 2733

## Online Material

**Table 2.** The KS test for the variation effects on *Fermi* and non-*Fermi* BL Lacs

Mode	$\delta$			$F_{\text{core}}$		
	KS statistic	probability	Significantly different	KS statistic	probability	Significantly different
$F120^a$	0.446	8.0e-08	YES	0.459	2.9e-08	YES
$F150^a$	0.413	8.7e-07	YES	0.459	2.9e-08	YES
$F200^a$	0.353	4.5e-05	YES	0.481	4.5e-09	YES
$F120^b$	0.441	1.1e-07	YES	0.459	2.9e-08	YES
$F150^b$	0.414	7.9e-07	YES	0.443	9.6e-08	YES
$F200^b$	0.373	1.3e-05	YES	0.441	1.1e-07	YES
$L120^a$	0.450	6.0e-08	YES	0.471	1.0e-08	YES
$L150^a$	0.441	1.1e-07	YES	0.451	5.0e-08	YES
$L200^a$	0.433	2.0e-07	YES	0.470	1.1e-08	YES
$L120^b$	0.453	4.5e-08	YES	0.467	1.4e-08	YES
$L150^b$	0.443	9.6e-08	YES	0.467	1.4e-08	YES
$L200^b$	0.391	3.8e-06	YES	0.456	3.6e-08	YES
$R120^a$	0.470	1.1e-08	YES	0.467	1.4e-08	YES
$R150^a$	0.477	6.4e-09	YES	0.487	2.8e-09	YES
$R200^a$	0.453	4.5e-08	YES	0.487	2.8e-09	YES
$R120^b$	0.449	6.2e-08	YES	0.471	1.0e-08	YES
$R150^b$	0.436	1.7e-07	YES	0.461	2.9e-08	YES
$R200^b$	0.401	1.9e-06	YES	0.464	1.8e-08	YES

Notes: F120, F150, and F200 - a subsample of sources with the highest radio core flux, are assumed to be at elevated state with radio core flux at 120%, 150%, and 200% of the quiescent state, respectively; L120, L150, and L200: a subsample of sources with the highest radio core luminosity, are assumed to be at elevated state with radio core luminosity at 120%, 150%, and 200% of the quiescent state, respectively; R120, R150, and R200: a subsample of random sources are assumed to be at elevated state of 120%, 150%, and 200% of the quiescent state, respectively. <sup>a</sup> and <sup>b</sup> indicate that the subsample size are 30%, and 50% of the whole sample, respectively.

**Fig. 6.** The distributions of Doppler factor  $\delta$  for LBL( top Left), IBL(top right) and HBLs(bottom). The dashed lines are for FBLs, while the solid lines for NFBLs.



**Table 3.** The sample of 170 BL Lac objects in Wu et al. (2007).

IAU name	Source	$z$	$\nu'_{\text{peak}}$ [Hz]	$\log P_{408 \text{ M}}$ [Jy]	$F_{\text{core}}$ [Jy]	$\delta$	$P_{\text{NVSS}}$	$M_{\text{host}}$	Class	$F_{\gamma}$ [erg/cm <sup>2</sup> /s]	$\beta_{\text{app}}$	Ref.
(1)	(2)	(3)	(4)	(5)	(6)	(7)	(8)	(9)	(10)	(11)	(12)	
0006-063	NRAO 5	0.347	12.10	26.94	1.492	5.97	2.69	...	NFBL	...	2.89	1
0007+472	RX J0007.9+4711	2.100	15.99	27.68	0.067	4.40	1.08	-27.08	FBL	0.24E-10	...	...
0035+598	1ES 0033+595	0.086	18.60	24.01	0.062	2.33	0.66	-20.41	FBL	0.29E-10	...	...
0040+408	1ES 0037+405	0.271*	16.62	24.93	0.015	1.92	...	...	NFBL	...	...	...
0050-094	PKS 0048-097	0.635	12.94	27.47	0.537	4.58	3.13	...	FBL	0.43E-10	13.80	2
0110+418	NPM1G +41.0022	0.096	17.72	24.41	0.018	1.06	3.64	-22.94	NFBL	...	...	...
0112+227	S2 0109+22	0.265	12.84	25.77	0.700	7.09	8.47	...	FBL	0.79E-10	...	...
0115+253	RXS J0115.7+2519	0.350	13.15	25.31	0.027	2.59	...	-23.44	FBL	0.14E-10	...	...
0123+343	1ES 0120+340	0.272	17.96	24.86	0.031	2.93	2.41	-23.30	FBL	0.58E-11	...	...
0124+093	MS 0122.1+0903	0.339	15.36	23.58	0.001	1.96	...	-23.07	NFBL	...	...	...
0136+391	B3 0133+388	0.271*	16.31	25.44	0.049	2.44	0.83	...	FBL	0.62E-10	...	...
0141-094	PKS 0139-09	0.735	12.77	27.18	0.696	7.43	1.50	-25.19	FBL	0.18E-10	5.50	3
0148+140	1ES 0145+138	0.125	15.76	24.22	0.002	0.54	1.35	-22.17	NFBL	...	...	...
0153+712	8C 0149+710	0.022	14.65	23.99	0.291	1.29	3.10	-23.23	NFBL	...	...	...
0201+005	MS 0158.5+0019	0.299	17.62	24.47	0.009	2.30	1.97	-23.11	NFBL	...	...	...
0208+353	MS 0205.7+3509	0.318	14.90	23.91	0.005	2.75	8.30	...	NFBL	...	...	...
0214+517	87GB 02109+5130	0.049	17.53	24.50	0.161	1.50	4.32	-23.13	NFBL	...	...	...
0222+430	3C 66A	0.440	15.20	27.55	0.916	3.85	1.75	...	FBL	0.26E-09	19.30	4
0232+202	1ES 0229+200	0.140	19.22	24.75	0.045	1.93	2.15	-23.77	NFBL	...	...	...
0238+166	AO 0235+164	0.940	12.82	27.24	0.972	10.78	1.47	-26.76	FBL	0.18E-09	25.60	5
0301+346	MS 0257.9+3429	0.245	13.10	24.49	0.009	1.90	5.35	-23.28	NFBL	...	...	...
0314+247	RXS J0314.0+2445	0.054	12.71	22.95	0.006	0.96	1.52	-21.26	NFBL	...	...	...
0326+024	2E 0323+0214	0.147	19.61	24.16	0.020	2.07	3.03	-22.63	FBL	0.14E-10	...	...
0416+010	2E 0414+0057	0.287	20.49	25.70	0.048	2.13	2.22	-24.02	FBL	0.78E-11	1.81	6
0422+198	MS 0419.3+1943	0.512	16.63	25.15	0.008	2.32	3.64	-23.54	NFBL	...	...	...
0424+006	PKS 0422+004	0.268	15.02	26.19	0.872	5.95	2.18	...	FBL	0.23E-10	...	...
0505+042	RXS J0505.5+0416	0.027	16.87	23.56	0.090	1.20	1.72	-17.55	FBL	0.85E-11	...	...
0507+676	1ES 0502+675	0.340	18.55	24.28	0.033	5.77	2.44	...	FBL	0.42E-10	...	...
0508+845	S5 0454+84	1.340	12.60	26.28	0.533	22.37	0.30	-22.89	NFBL	...	...	...
0509-040	4U 0506-03	0.304	17.77	25.57	0.029	1.93	1.12	-23.23	NFBL	...	...	...
0613+711	MS 0607.9+7108	0.267	14.41	24.03	0.014	3.49	1.94	-23.67	NFBL	...	...	...
0625+446	87GB 06216+4441	0.311	13.05	25.83	0.248	4.80	4.70	...	FBL	0.95E-11	...	...
0650+250	1ES 0647+250	0.203	17.85	24.85	0.069	3.24	0.25	-21.39	FBL	0.27E-10	...	...
0654+427	B3 0651+428	0.126	14.80	25.07	0.134	2.38	2.32	-23.27	NFBL	...	...	...
0656+426	NPM1G +42.0131	0.059	17.34	25.85	0.253	0.86	2.21	-23.48	NFBL	...	...	...
0710+591	EXO 0706.1+5913	0.125	20.83	25.03	0.080	1.87	0.32	-23.27	FBL	0.13E-10	6.87	7
0721+713	S5 0716+714	0.300	14.06	26.50	0.315	3.23	2.34	-21.41	FBL	0.18E-09	14.80	4
0738+177	PKS 0735+17	0.424	12.64	25.43	2.775	29.41	2.17	-22.08	FBL	0.57E-10	7.40	3
0744+745	MS 0737.9+7441	0.315	13.24	24.75	0.021	3.05	...	-23.53	FBL	0.77E-11	...	...
0753+538	S4 0749+54	0.200	12.23	25.47	1.390	9.26	2.87	-18.51	FBL	0.13E-10	...	...
0757+099	PKS 0754+100	0.266	12.48	25.25	2.073	17.72	4.49	-22.34	FBL	0.23E-10	14.40	1
0806+595	SBS 0802+596	0.300	16.43	25.26	0.029	2.36	...	-24.32	NFBL	...	...	...
0809+523	1ES 0806+524	0.137	16.09	24.90	0.172	3.32	3.04	-23.22	FBL	0.28E-10	...	...
0818+423	OJ 425	0.530	12.71	27.20	1.011	6.33	2.82	-21.95	FBL	0.81E-10	4.90	8
0823+223	4C 22.21	0.951	12.94	28.53	0.388	2.73	1.22	-24.87	NFBL	...	...	...
0825+031	PKS 0823+033	0.505	11.79	25.23	1.453	29.41	5.22	-23.01	FBL	0.76E-11	17.80	1
0831+044	PKS 0829+046	0.174	12.81	25.74	1.230	6.21	3.51	-22.96	FBL	0.47E-10	10.10	1
0831+087	1H 0827+089	0.941	13.90	26.67	0.061	4.04	0.27	...	NFBL	...	...	...
0832+492	OJ 448	0.548	12.33	25.98	0.294	8.39	3.45	-23.24	NFBL	...	6.30	3
0854+441	US 1889	0.382	17.31	26.05	0.031	1.79	...	...	NFBL	...	...	...

Continued...

IAU name	Source	$z$	$\nu'_{\text{peak}}$ [Hz]	$\log P_{408 \text{ M}}$ [Jy]	$F_{\text{core}}$ [Jy]	$\delta$	$P_{\text{NVSS}}$	$M_{\text{host}}$	Class	$F_{\gamma}$ [erg/cm <sup>2</sup> /s]	$\beta_{\text{app}}$	Ref.
(1)	(2)	(3)	(4)	(5)	(6)	(7)	(8)	(9)	(10)	(11)	(12)	
0854+201	OJ 287	0.306	12.75	25.25	1.557	17.87	8.19	-22.93	FBL	0.41E-10	15.17	1
0915+295	B2 0912+29	0.302*	15.64	26.20	0.172	2.96	1.29	...	FBL	0.25E-10	...	...
0916+526	RXS J0916.8+5238	0.190	17.03	25.26	0.046	1.85	0.86	-23.88	NFBL	...	...	...
0929+502	RXS J0929.2+5013	0.370	13.76	26.08	0.916	9.23	3.32	...	FBL	0.81E-11	...	...
0930+498	1ES 0927+500	0.188	20.77	24.06	0.018	2.70	1.29	-22.44	NFBL	...	...	...
0930+350	B2 0927+35	0.302*	14.35	26.48	0.394	3.68	0.70	...	NFBL	...	...	...
0952+656	RGB J0952+656	0.302*	14.90	25.46	0.027	1.99	4.95	...	NFBL	...	...	...
0954+492	MS 0950.9+4929	0.380	16.73	24.20	0.003	2.12	11.15	...	NFBL	...	...	...
0958+655	S4 0954+65	0.368	13.06	25.66	0.276	6.79	5.81	-22.66	FBL	0.18E-10	6.20	3
1012+424	RXS J1012.7+4229	0.365	20.82	25.83	0.029	1.92	0.61	-23.84	FBL	0.44E-11	...	...
1015+494	GB 1011+496	0.212	16.40	25.85	0.173	2.64	1.97	-23.95	FBL	0.73E-10	...	...
1031+508	1ES 1028+511	0.360	18.16	25.32	0.044	3.39	1.28	-23.32	FBL	0.14E-10	...	...
1037+571	RXS J1037.7+5711	0.830	14.52	26.48	0.089	4.94	0.65	...	FBL	0.33E-10	...	...
1047+546	1ES 1044+549	0.540	12.86	24.82	0.004	2.13	...	-23.15	NFBL	...	...	...
1053+494	MS 1050.7+4946	0.140	14.95	24.30	0.040	2.49	...	-23.98	FBL	0.12E-10	...	...
1104+382	MRK 421	0.030	18.20	24.37	0.639	1.99	2.20	-22.38	FBL	0.38E-09	0.80	8
1109+241	1ES 1106+244	0.482	16.69	25.55	0.018	2.45	1.49	-23.31	FBL	0.40E-11	...	...
1120+422	EXO 1118.0+4228	0.124	17.22	24.10	0.019	1.76	1.91	...	FBL	0.18E-10	...	...
1136+701	MRK 180	0.045	18.74	25.14	0.131	0.78	2.33	-22.13	FBL	0.15E-10	2.23	6
1136+676	RXS J1136.5+6737	0.134	17.18	24.16	0.040	2.64	3.64	-23.24	FBL	0.84E-11	...	...
1149+246	EXO 1449.9+2455	0.402	19.63	25.32	0.015	2.20	2.01	-23.58	NFBL	...	...	...
1150+242	B2 1147+245	0.200	13.18	25.30	0.638	7.11	1.91	-19.56	FBL	0.15E-10	...	...
1151+589	RXS J1151.4+5859	0.302*	16.10	25.98	0.095	2.58	1.05	...	FBL	0.96E-11	...	...
1209+413	B3 1206+416	0.377	13.87	25.87	0.397	7.19	2.23	...	FBL	0.67E-11	...	...
1215+075	1ES 1212+078	0.136	15.57	24.84	0.091	2.49	2.19	-23.22	NFBL	...	...	...
1217+301	B2 1215+30	0.130	15.10	25.46	0.445	3.39	5.38	-23.15	FBL	0.61E-10	1.19	6
1220+345	GB2 1217+348	0.643	13.91	26.64	0.258	5.80	1.16	...	NFBL	...	...	...
1221+301	PG 1218+304	0.184	18.80	24.88	0.056	2.61	0.69	-22.90	FBL	0.38E-10	...	...
1221+282	ON 231	0.103	14.15	25.13	1.117	5.34	2.85	-21.95	FBL	0.62E-10	3.20	8
1223+806	S5 1221+80	0.430	13.74	26.89	0.447	4.20	1.45	...	FBL	0.13E-10	...	...
1224+246	MS 1221.8+2452	0.218	13.60	24.25	0.021	2.96	2.08	-21.84	FBL	0.70E-11	...	...
1230+253	RXS J1230.2+2517	0.135	14.40	25.26	0.351	3.60	2.70	...	FBL	0.11E-10	...	...
1231+642	MS 1229.2+6430	0.163	15.84	24.32	0.042	2.96	3.93	-23.32	NFBL	...	...	...
1237+629	MS 1235.4+6315	0.297	15.61	24.38	0.014	3.02	1.40	...	NFBL	...	...	...
1241+066	1ES 1239+069	0.150	17.05	23.48	0.010	2.45	2.67	-17.19	NFBL	...	...	...
1248+583	PG 1246+586	0.847	14.27	26.90	0.779	11.10	2.23	-24.23	FBL	0.47E-10	...	...
1253+530	S4 1250+53	0.663	14.39	27.26	0.346	4.44	2.46	...	FBL	0.42E-10	...	...
1257+242	1ES 1255+244	0.141	16.83	24.00	0.007	1.30	...	-22.59	NFBL	...	...	...
1310+325	AUCVn	0.996	12.61	26.53	2.107	27.73	1.60	-26.16	FBL	0.52E-10	20.88	9
1322+081	1ES 1320+084N	0.049	12.99	22.74	0.012	1.43	...	-17.98	NFBL	...	...	...
1341+399	RXS J1341.0+3959	0.169	19.97	25.22	0.034	1.45	...	-23.73	NFBL	...	...	...
1402+159	MC 1400+162	0.244	16.29	26.54	0.178	1.90	6.03	...	NFBL	...	...	...
1404+040	MS 1402.3+0416	0.344	15.74	25.76	0.021	1.64	...	-22.43	NFBL	...	...	...
1409+596	MS 1407.9+5954	0.496	16.40	25.50	0.017	2.55	1.88	-23.99	NFBL	...	...	...
1415+485	RGB J1415+485	0.496	14.13	25.72	0.058	4.06	2.03	-22.94	NFBL	...	...	...
1415+133	PKS 1413+135	0.247	12.39	26.67	0.694	3.47	0.10	...	FBL	0.72E-11	7.10	8
1417+257	2E 1415+2557	0.237	19.00	25.29	0.040	2.13	2.31	-24.10	FBL	0.50E-11	...	...
1419+543	OQ 530	0.152	13.16	24.67	1.188	11.38	1.25	-23.40	FBL	0.98E-11	3.60	3
1427+238	PKS 1424+240	0.300	15.30	26.31	0.250	3.29	1.12	-20.29	FBL	0.14E-09	...	...
1427+541	RGB J1427+541	0.106	14.79	24.38	0.024	1.38	...	-23.64	NFBL	...	...	...
1428+426	H 1426+428	0.129	18.41	24.43	0.022	1.56	1.07	-22.94	FBL	0.17E-10	...	...
1439+395	PG 1437+398	0.260	16.57	25.70	0.038	1.71	1.73	-23.12	FBL	0.56E-11	...	...
1442+120	1ES 1440+122	0.163	16.20	24.81	0.041	2.06	1.32	-23.01	FBL	0.89E-11	...	...

Continued...

IAU name	Source	$z$	$\nu'_{\text{peak}}$ [Hz]	$\log P_{408 \text{ M}}$ [Jy]	$F_{\text{core}}$ [Jy]	$\delta$	$P_{\text{NVSS}}$	$M_{\text{host}}$	Class	$F_{\gamma}$ [erg/cm <sup>2</sup> /s]	$\beta_{\text{app}}$	Ref.
(1)	(2)	(3)	(4)	(5)	(6)	(7)	(8)	(9)	(10)	(11)	(12)	
1444+636	MS 1443.5+6349	0.298	16.94	24.31	0.004	1.69	4.66	...	NFBL	...	...	...
1448+361	RXS J1448.0+3608	0.738	16.44	26.06	0.029	3.38	...	...	FBL	0.14E-10	...	...
1458+373	B3 1456+375	0.333	12.86	25.91	0.305	5.38	6.11	...	NFBL	...	...	...
1501+226	MS 1458.8+2249	0.235	14.69	24.73	0.085	4.59	3.48	-22.95	FBL	0.24E-10	...	...
1509+559	SBS 1508+561	2.025	15.00	26.84	0.028	5.03	2.85	...	FBL	0.50E-11	...	...
1516+293	RXS J1516.7+2918	0.130	18.56	25.01	0.034	1.29	2.57	-23.41	NFBL	...	...	...
1517+654	1H 1515+660	0.702	17.82	25.72	0.019	3.32	0.46	-24.64	FBL	0.98E-11	...	...
1532+302	RXS J1532.0+3016	0.064	16.86	23.87	0.047	1.66	2.08	-22.43	NFBL	...	...	...
1533+342	RXS J1533.4+3416	0.810	17.89	25.77	0.033	4.86	1.19	...	NFBL	...	...	...
1534+372	RGB J1534+372	0.144	13.97	24.03	0.020	2.22	4.82	-22.20	FBL	<b>0.51E-11</b>	...	...
1535+533	1ES 1533+535	0.890	19.55	25.97	0.010	2.55	4.44	-26.35	NFBL	...	...	...
1536+016	MS 1534.2+0148	0.312	18.67	25.53	0.025	1.89	1.65	-23.43	NFBL	...	...	...
1540+819	1ES 1544+820	0.271*	17.53	25.42	0.043	2.30	2.33	-21.56	FBL	0.73E-11	...	...
1540+147	4C 14.6	0.605	14.25	27.58	1.329	6.34	3.10	-24.00	FBL	<b>0.63E-11</b>	8.73	1
1542+614	RXS J1542.9+6129	0.302*	14.19	25.27	0.102	4.42	1.33	...	FBL	0.72E-10	...	...
1554+201	MS 1552.1+2020	0.222	16.89	25.09	0.032	2.06	3.04	-23.77	NFBL	...	...	...
1555+111	PG 1553+11	0.360	15.92	26.29	0.398	5.07	1.60	-20.42	FBL	0.20E-09	...	...
1602+308	RXS J1602.2+3050	1.091	16.32	26.70	0.020	2.63	1.78	...	NFBL	...	...	...
1626+352	RXS J1626.4+3513	0.497	15.05	25.39	0.014	2.53	...	-24.36	NFBL	...	...	...
1644+457	RXS J1644.2+4546	0.225	17.28	25.67	0.064	1.95	1.88	-23.50	NFBL	...	...	...
1652+403	RGB J1652+403	0.240	14.80	24.60	0.011	1.85	...	...	NFBL	...	0.54	6
1653+397	MRK 501	0.034	16.17	23.79	1.251	4.79	1.37	-23.36	FBL	0.11E-09	1.50	4
1704+716	RXS J1704.8+7138	0.350	15.32	25.06	0.017	2.45	2.06	-22.83	NFBL	...	...	...
1719+177	PKS 1717+177	0.137	12.43	25.19	0.601	5.03	3.70	...	FBL	0.27E-10	...	...
1724+400	B2 1722+40	1.049	12.64	27.81	0.341	4.72	0.62	...	FBL	0.26E-10	...	...
1725+118	H 1722+119	0.018	15.76	23.06	0.088	1.13	0.56	-13.71	FBL	0.42E-10	...	...
1728+502	IZw187	0.055	17.16	24.20	0.134	1.91	3.99	-21.60	FBL	0.97E-11	5.30	6
1739+476	OT 465	0.950	13.39	27.86	0.848	6.50	2.47	-24.21	FBL	0.63E-11	...	...
1742+597	RGBJ 1742+597	0.400	13.75	25.73	0.077	3.73	1.40	-23.01	FBL	0.61E-11	...	...
1743+195	NPM1G +19.0510	0.084	17.44	24.40	0.210	3.19	1.20	-23.77	FBL	0.94E-11	1.17	6
1745+398	B3 1743+398B	0.267	17.58	26.55	0.118	1.69	0.86	-24.45	NFBL	...	...	...
1747+469	B3 1746+470	1.484	13.30	27.26	0.456	11.33	1.87	...	NFBL	...	...	...
1748+700	S4 1749+70	0.770	13.80	26.63	0.521	9.94	2.24	-25.72	FBL	0.24E-10	3.20	3
1749+433	B3 1747+433	0.571	13.08	26.82	0.281	4.71	5.82	...	FBL	0.15E-10	...	...
1750+470	RXS J1750.0+4700	0.160	18.31	25.28	0.010	0.72	...	-23.09	NFBL	...	...	...
1751+096	PKS 1749+096	0.322	11.33	24.92	3.796	37.09	2.00	-23.20	FBL	0.41E-10	6.84	9
1756+553	RXS J1756.2+5522	0.657	19.74	25.63	0.010	2.40	0.51	...	FBL	0.68E-11	...	...
1757+705	MS 1757.7+7034	0.407	13.37	24.65	0.011	3.02	...	-22.80	NFBL	...	...	...
1800+784	S5 1803+784	0.680	13.35	27.57	1.878	8.51	3.48	-23.56	FBL	0.52E-10	8.97	1
1806+698	3C 371	0.051	14.42	25.87	1.508	1.79	3.33	-22.71	FBL	0.44E-10	2.90	8
1808+468	RGB J1808+468	0.450	14.34	25.85	0.041	2.80	0.98	-22.77	NFBL	...	...	...
1811+442	RGB J1811+442	0.350	15.30	25.92	0.006	0.79	1.19	-23.77	NFBL	...	...	...
1813+317	B2 1811+31	0.117	15.34	25.00	0.074	1.73	2.48	-21.02	FBL	0.20E-10	...	...
1824+568	4C 56.27	0.664	12.56	28.02	0.859	4.07	1.56	-24.13	FBL	0.36E-10	20.85	1
1829+540	RXS J1829.4+5402	0.302*	15.06	25.73	0.018	1.34	1.57	...	FBL	0.80E-11	...	...
1838+480	RXS J1838.7+4802	0.300	13.24	25.05	0.023	2.45	2.13	-22.35	FBL	0.16E-10	...	...
1841+591	RGB J1841+591	0.530	14.94	25.68	0.006	1.44	...	-24.33	NFBL	...	...	...
1853+672	1ES 1853+671	0.212	16.25	23.81	0.012	3.00	6.79	-22.27	NFBL	...	...	...
1927+612	S4 1926+61	0.473*	12.72	26.62	0.826	7.66	2.42	...	FBL	0.95E-11	...	...
1959+651	1ES 1959+650	0.047	17.33	23.01	0.252	5.20	1.42	-22.20	FBL	0.67E-10	...	...
2005+778	S5 2007+77	0.342	12.39	26.14	0.822	7.70	1.46	-23.13	FBL	0.12E-10	2.90	3
2009+724	S5 2010+72	1.740	13.08	28.41	1.390	10.02	1.35	...	FBL	0.18E-10	...	...
2022+761	S5 2023+76	0.594	13.54	26.89	0.425	5.75	2.42	...	FBL	0.19E-10	...	...

Continued...

IAU name	Source	$z$	$\nu'_{\text{peak}}$ [Hz]	$\log P_{408 \text{ M}}$ [Jy]	$F_{\text{core}}$ [Jy]	$\delta$	$P_{\text{NVSS}}$	$M_{\text{host}}$	Class	$F_{\gamma}$ [erg/cm <sup>2</sup> /s]	$\beta_{\text{app}}$	Ref.
(1)	(2)	(3)	(4)	(5)	(6)	(7)	(8)	(9)	(10)	(11)	(12)	
2039+523	1ES 2037+521	0.053	15.60	22.27	0.032	3.55	...	-23.22	FBL	0.69E-11	...	...
2134-018	PKS 2131-021	1.285	12.04	27.93	1.733	11.93	1.19	-25.83	FBL	0.12E-10	7.70	8
2145+073	MS 2143.4+0704	0.237	13.61	25.14	0.045	2.53	1.21	-22.96	NFBL	...	...	...
2152+175	PKS 2149+17	0.874	13.03	26.67	0.648	12.23	1.06	-23.11	FBL	0.64E-11	...	...
2202+422	BL LAC	0.070	13.15	24.22	4.857	14.47	0.80	-23.08	FBL	0.11E-09	6.50	8
2250+384	B3 2247+381	0.119	15.35	24.65	0.060	2.03	3.03	-23.21	FBL	0.13E-10	...	...
2257+077	PKS 2254+074	0.190	13.31	24.78	0.525	8.85	4.89	-23.61	NFBL	...	4.30	3
2319+161	Q J2319+161	0.302*	15.30	25.14	0.017	2.00	3.03	...	NFBL	...	...	...
2322+346	TEX 2320+343	0.098	16.68	24.58	0.030	1.23	...	-23.39	FBL	0.56E-11	...	...
2323+421	1ES 2321+419	0.268	12.90	24.52	0.019	2.90	2.57	...	FBL	0.30E-10	...	...
2329+177	1ES 2326+174	0.213	17.84	24.64	0.018	2.04	3.03	-22.94	NFBL	...	...	...
2339+055	MS 2336.5+0517	0.740	14.89	25.74	0.005	1.82	...	...	NFBL	...	...	...
2347+517	1ES 2344+514	0.044	15.86	23.30	0.212	3.63	0.62	-23.06	FBL	0.21E-10	1.15	6
2350+196	MS 2347.4+1924	0.515	15.72	24.80	0.003	1.81	...	...	NFBL	...	...	...

Notes: Col.4-7 were first reported in Wu et al. (2007), Col. 9 was first reported in Wu et al. (2009) and these values have been revised using redshift from Col 3. The columns are: Col. 1: the source IAU name (J2000). Col. 2: the source alias name. Col. 3: the redshift. ‘\*’ indicate that the redshift is unknown, and taken as the average redshift of LBL/IBL/HBL subclass. Col. 4: the synchrotron peak frequency. Col. 5: the total radio power at 408 MHz. Col. 6: The arcsecond scale radio flux at 5 GHz. Col. 7: the Doppler factor. Col. 8: the polarization fraction from NVSS in per cent. Col. 9: Absolute Magnitude of host galaxies. Col. 10, Indication of FBLs and NFBLs. Col. 11, observed  $\gamma$ -ray flux from 2nd year *Fermi*/LAT catalogue[100 MeV to 100 GeV]. Col. 12: the proper motion from literatures. Col. 13, the references of proper motion: 1. Kharb et al. (2010) 2. Piner et al. (2012) 3. Gabuzda et al. (2000) 4. Jorstad et al. (2001) 5. Piner et al. (2006) 6. Kharb et al. (2008) 7. Wu et al. (2012) 8. Kellermann et al. (2004) 9. Lister et al. (2009)